

## COMPUTER SIMULATION OF HIGH-TEMPERATURE CORROSION PHENOMENA

**Vicente Braz Trindade**

Universität Siegen, Institut für Werkstofftechnik, Paul-Bonatz Str. 9-11, 57068-Siegen, Germany  
[vicente@ifwt.mb.uni-siegen.de](mailto:vicente@ifwt.mb.uni-siegen.de)

**Ulrich Krupp**

[krupp@ifwt.mb.uni-siegen.de](mailto:krupp@ifwt.mb.uni-siegen.de)

**Udo Buschmann**

[buschmann@simtec.mb.uni-siegen.de](mailto:buschmann@simtec.mb.uni-siegen.de)

**Robert Orosz**

[orosz@ifwt.mb.uni-siegen.de](mailto:orosz@ifwt.mb.uni-siegen.de)

**Hans-Jürgen Christ**

[christ@ifwt.mb.uni-siegen.de](mailto:christ@ifwt.mb.uni-siegen.de)

**Abstract.** The aim of this paper is to introduce a computer simulation tool, which is designed for prediction of service-life of components operating under corrosive conditions such as carburization, oxidation and nitridation at high-temperature. Many laboratory experiments were carried out for the verification of the simulation results. Different classes of materials (low-Cr ferritic steels, austenitic steels and Ni-base superalloys) were exposed at temperatures between 550°C and 1000°C to different corrosive atmospheres (carburizing, oxidizing and nitriding). The tool for the prediction of internal/inwards corrosion processes at high-temperatures makes use of the numerical finite-difference technique to treat diffusional kinetics on the one hand and the concept of local equilibrium thermodynamics on the other hand. For this purpose, a link has been established between the numerical environment of MATLAB and the thermodynamic library ChemApp. Using this new tool, the kinetics of nitridation, oxidation and carburization processes were predicted numerically taking the material's microstructure into consideration by distinguishing between precipitation along the grain boundaries and within the grain interior. Excellent agreement between experimental observations and simulation results revealed the high potential of the computer modeling for application to complex corrosion processes.

**Keywords:** thermodynamics and diffusion simulation, oxidation, nitridation, carburization, finite-difference method

### 1. Introduction

Many industrial processes involve chemical reactions, that are thermally activated, consequently, operated at high-temperature conditions. In the petrochemical industry, for instance, large hydrocarbon molecules have to be cracked into small molecules, e.g., methane, ethylene, etc. These reactions take place in steel tubes located in a gas-fired furnace at temperatures up to 900°C. The surfaces of the tubes (reaction chambers) are exposed to high carbon activities. The soluble carbon can diffuse into the steel forming internal carbides (Grabke, 1998). Due to the higher carbon diffusion along grain boundaries, precipitation occurs preferentially intercrystalline. This phenomenon called carburization shortens the service-life of the tubes by degradation of its mechanical properties.

In the power generation industry, steels are also used as boiler materials. The operation temperature in the different components of a boiler system varies from 400°C to 650°C. The tubes are exposed to an outer oxidizing atmosphere and internally to very high pressures (up to 300 bar). Therefore, the performance of the boiler components is strongly dependent on their resistance to oxidation, since the formation of oxide scales causes a reduction of the thickness of the tube walls. Usually, the oxidation rate of steels is strongly dependent on their chromium content, because chromium has a very high affinity to oxygen, i.e., chromium oxide ( $\text{Cr}_2\text{O}_3$ ) has a high thermodynamic stability. Its very low defect density results in an adherent, slow-growing, and protective scale (Kofstad, 1966).

In the aeronautic industry, critical components subject to failure caused by high temperature corrosion are the turbine blades, which are made of Ni-base superalloys. The very high temperatures (up to 1100°C), at which the turbine blades are used represent very aggressive conditions, even when a chromia scale is formed on the surface. Under these conditions, elements such as oxygen and/or nitrogen can penetrate within the oxide scale and dissolve in the alloys causing internal precipitation of oxides and/or nitrides reducing the service-life of the blades (Krupp, 2000).

The stability of the different phases such as carbides, oxides and nitrides can be evaluated by their thermodynamic properties. However, the existence of complex solid solution such as some carbides and oxides containing different metallic elements in its sublattices, a proper prediction of phase equilibrium becomes reasonable when using computational thermochemistry. Besides thermodynamics, the kinetics of the corrosion process has to be evaluated by considering that the most of the corrosion phenomena are controlled by solid state diffusion. Therefore, the diffusion of

the different species participating in the corrosion phenomena must be taken into account and considering the high diffusivity along grain boundaries.

In this paper both thermodynamics and diffusion characteristics of the different corrosion degradation phenomena are considered. Computational thermodynamics is done by means of the powerful programmable thermochemical subroutine ChemApp by GTT Technologies using tailored thermodynamic data bank for steels and Ni-base superalloys. The kinetic calculations are performed by solving the diffusion differential equation in one- and two-dimensional cases with help of the finite-difference method. A computer tool for description of high-temperature corrosion phenomena is presented and the simulation results are compared with that experimentally observed.

### 3. Materials and experimental procedure

In this paper three classes of materials are considered: (i) low-Cr ferritic steels used in power plant, (ii) austenitic steels used in petrochemical industry and (iii) Ni-base superalloys used in the aeronautic industry. The low-alloy steels have chromium content from 0.5wt.% to 2.25wt.% and they were oxidized in laboratory air at 550°C. The austenitic steel containing 16.8wt.% of Cr and 7.41wt.% of nickel was exposed to an oxygen-free He atmosphere containing 1vol% of methane at 850°C. One of the Ni-base superalloys (IN625) was exposed to laboratory air at a temperature range between 850°C and 1000°C. The Ni-base superalloy Nicrofer7520Ti was exposed to nitriding/oxidizing atmospheres at 1000°C. The chemical composition of the materials used are given in Table 1.

The materials were isothermally exposed to high temperatures and the mass change during the different corrosion processes was recorded using a microbalance with a resolution of  $10^{-5}$ g connected to a computer. The oxide, nitride and carbide phases were analyzed using scanning electron microscopy (SEM) in combination with energy-dispersive X-ray spectroscopy (EDX).

Table 1. Chemical compositions (in wt.%) of the materials used.

Alloy	C	Cr	Mo	Ti	Al	Si	Ni	Fe
71518	0.07	0.55	---	---	---	---	---	bal.
NrX60	0.06	1.44	---	---	---	---	---	bal.
2.25Cr1Mo	0.09	2.25	1	---	---	---	---	bal.
AISI 301	0.108	16.8	0.32	---	0.033	0.98	7.41	bal.
IN625	0.01	19.0	8.9	0.28	0.24	1.20	bal.	2.80
Nicrofer7520	0.02	20.2	---	2.7	1.6	---	bal.	0.2

### 4. Computer simulation

Generally, the driving force of high-temperature corrosion processes can be separated into (i) transport mechanisms, i.e., solid-state diffusion, and (ii) thermodynamics of chemical reactions. The commonly used, phenomenological way to treat diffusion processes is the application of a second-order partial differential equation (Fick's 2<sup>nd</sup> law) formulating a relationship between the derivative of the concentration of a species  $c$  after the time  $t$  and its gradient by means of the location- and temperature-dependent diffusion coefficient  $D$ .

$$\frac{\partial c}{\partial t} = D \frac{\partial^2 c}{\partial x^2} \quad (1)$$

The use of analytical solutions for Eq. (1) to describe the corrosion phenomena in complex situations is widely limited. Therefore, numerical methods, e.g. the finite-difference technique, has the advantage that the concentrations of the species can be calculated in discrete steps of time and location. Such approaches the incorporation of computational thermodynamics in each of the discrete steps.

The basic idea of the finite-difference method to solve partial differential equations is to replace spatial and time derivatives by suitable approximations and then to numerically solve the resulting difference equations. In other words, instead of solving for  $c(x, t)$  with  $x$  and  $t$  continuous, it is solved for  $c_{i,j} = c(x_i, t_j)$ , where  $x_i = i\Delta x$  and  $t_j = j\Delta t$ . Thus, if all the concentrations are known at time  $t_j$ , then one step of the process is to determine them at time  $t_{j+1} = t_j + \Delta t$ . If this can be done, then, given the initial state, the concentration profiles can be determined for all following time steps. Using the Crank-Nicolson technique (Crank, 1986,) Eq.(1) can be approximated as follows

$$\frac{\partial c}{\partial t} \cong \frac{c_i^{j+1} - c_i^j}{\Delta t} \quad (2)$$

$$\frac{\partial^2 c}{\partial x^2} \cong \frac{1}{2} \left( \frac{c_{i+1}^{j+1} - 2c_i^{j+1} + c_{i-1}^{j+1}}{(\Delta x)^2} + \frac{c_{i+1}^j - 2c_i^j + c_{i-1}^j}{(\Delta x)^2} \right) \quad (3)$$

By combining Eq. (2) and Eq. (3) the concentrations  $c_i^{j+1}$  of the diffusing species for the location step  $i$  and the time step  $j+1$  are calculated from the neighbouring concentrations according to the Eq. (4) and schematically represented in Fig. 1.

$$c_i^{j+1} = c_i^j + \frac{D\Delta t}{2(\Delta x)^2} \left[ (c_{i+1}^{j+1} + c_{i+1}^j) - 2(c_i^{j+1} + c_i^j) + (c_{i-1}^{j+1} + c_{i-1}^j) \right] \quad (4)$$

For separation of diffusion along grain boundaries from that in the bulk, a two-dimensional calculation is required. In this case, the diffusion coefficient  $D$  is treated as a matrix containing the diffusion coefficients of the diffusing species as a function of the position  $x$  and  $y$ . This allows to change the diffusion coefficient locally, e.g., along grain boundaries.

Equation (1) is solved for all species participating in the corrosion process and stepwise for the complete reaction time  $p \cdot \Delta t$  using the commercial simulation environment MATLAB according to the schematic representation in Fig. 1 (simplified for one-dimensional diffusion). To account for possible chemical reactions of the ongoing corrosion process, the calculated concentrations at  $c_i^{j+1}$  must be corrected according to the local thermodynamic equilibrium. This becomes possible by transferring the concentration  $c_i^{j+1}$  into the thermodynamic subroutine ChemApp. ChemApp is based on a numerical Gibbs' energy minimization routine in combination with tailor-made data bases. The excessive computation time was drastically reduced by using the parallel computing system PVM (parallel virtual machine) (Krupp, 2005). Using this computation methodology the thermodynamic equilibrium calculations are distributed to individual thermodynamic workers according to the schematic representation in Fig. 1.

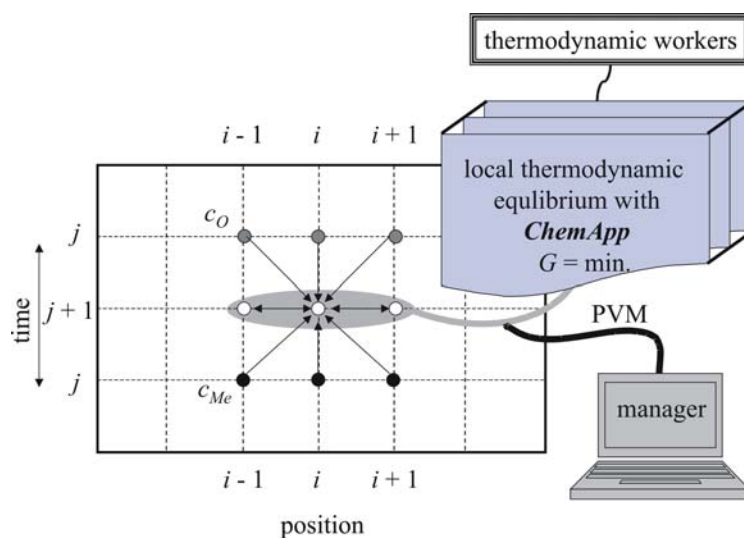


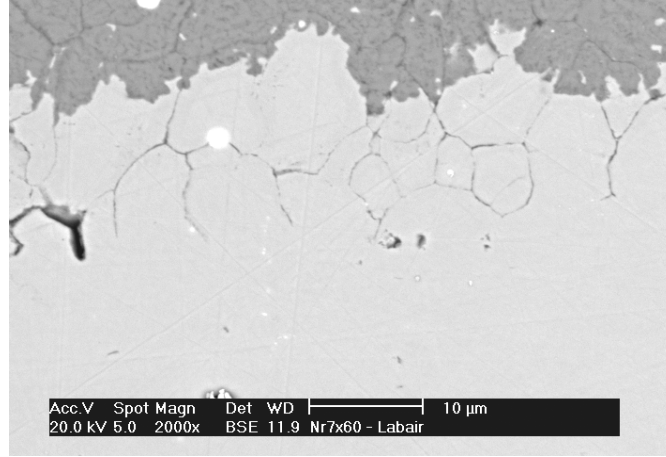
Figure 1. Schematic representation of the finite-difference technique (implicit Crank-Nicolson approach) in combination with the thermodynamic subroutine ChemApp.

## 5. Results and discussion

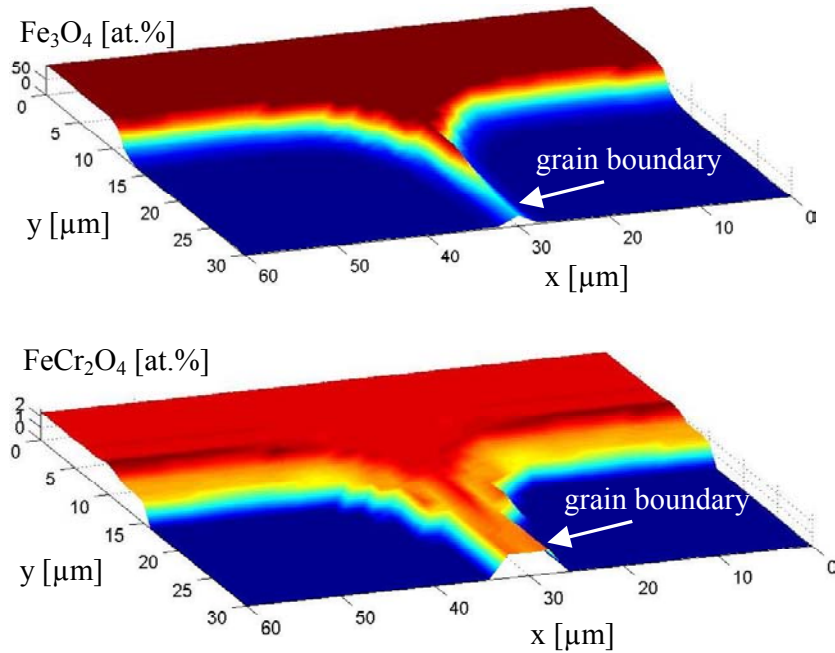
On the surface of the low-Cr ferritic steels a thick oxide scale was formed following parabolic rate law kinetics, strongly dependent on the microstructure (grain size) of the alloy. It has been shown by Trindade et al. (2005) that this oxide scale was composed of two layers: (i) an outer layer of magnetite ( $\text{Fe}_3\text{O}_4$ ) and hematite ( $\text{Fe}_2\text{O}_3$ ), which grows by outwards diffusion of iron and (ii) an inner layer of spinel ( $\text{FeFe}_{2-x}\text{Cr}_x\text{O}_4$ ) with stoichiometry varying from  $x=0$  (pure

magnetite –  $\text{Fe}_3\text{O}_4$ ) up to  $x=2$  (normal spinel –  $\text{FeCr}_2\text{O}_4$ ). The growth of the inner layer is determined by fast diffusion of oxygen along alloy grain boundaries resulting in an intergranular oxidation mechanism (see Fig. 2a).

The application of the developed simulation tool to the oxidation of low-Cr steels is demonstrated by calculations of the inner oxide scale growth. To account for the intercrystalline oxidation mechanism, the diffusion of oxygen and chromium along alloy grain boundaries was separated from that in the bulk. Figure 2b shows the simulated concentration profiles of  $\text{Fe}_3\text{O}_4$  and the complete spinel  $\text{FeCr}_2\text{O}_4$ . The high oxygen grain boundary diffusivity cause the primary formation of oxides along grain boundaries and the lateral diffusion from the grain boundary in the interior of the grain determines the kinetics of the inward oxidation of these steel grade.



(a)



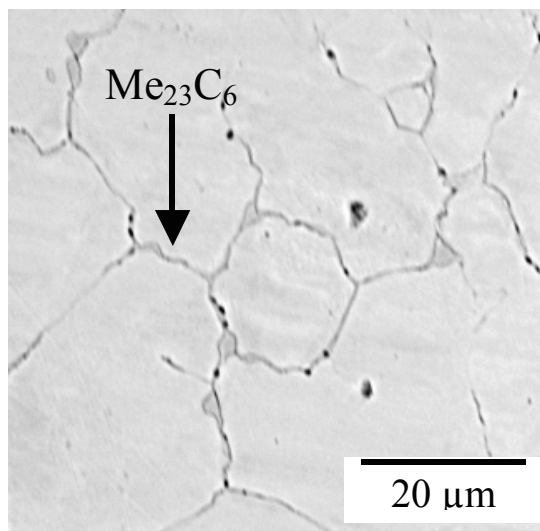
(b)

Figure 2. Oxide scale formed on low-Cr steel with a grain size of 30μm at 550°C exposed to laboratory air: (a) detail of the formation of inner oxide scale and (b) simulation of the intergranular growth of the inner scale.

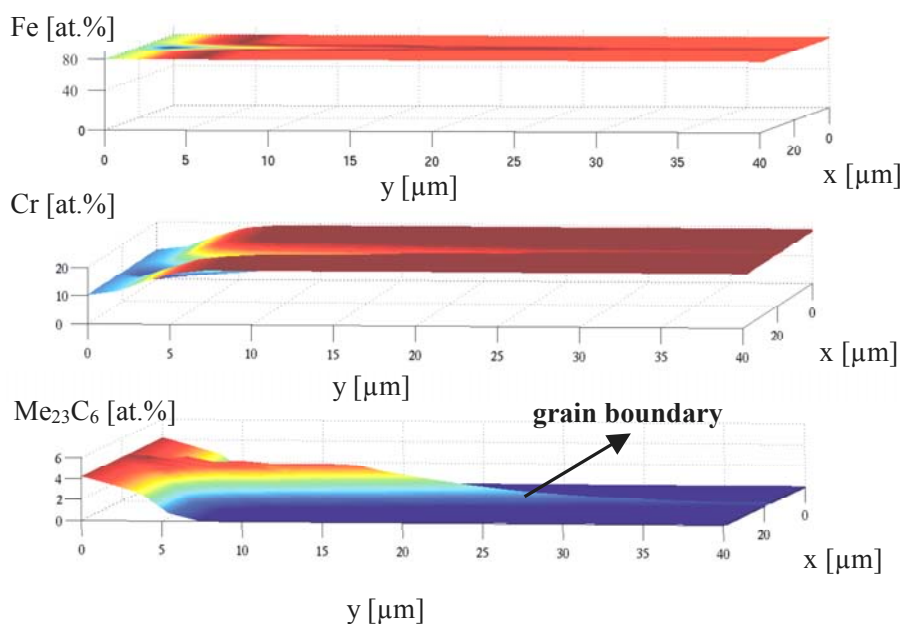
The exposure of the austenitic steel to a carburizing atmosphere causes the dissolution of carbon in the alloy and its diffusion into the alloy leads to formation of carbides. The high affinity of chromium and iron to carbon cause the formation of carbides such as  $\text{Me}_7\text{C}_3$  and  $\text{Me}_{23}\text{C}_6$ , where Me denotes the metallic component (Fe and Cr). The high diffusivity of carbon along alloy grain boundaries causes the formation of the most stable  $\text{Me}_{23}\text{C}_6$  carbide along grain boundaries, which transforms to  $\text{Me}_7\text{C}_3$  as the carbon activity increases. Figure 3a shows the formation of  $\text{Me}_{23}\text{C}_6$

formed during the first stage of exposure. An external oxide scale was not formed due to the very low oxygen partial pressure in the atmosphere.

Figure 3b shows the concentration profiles of the main species involved in the carburization process. The formation of  $\text{Me}_{23}\text{C}_6$  along grain boundaries and in the grain interior as well as the depletion of iron and chromium in the matrix and along alloy grain boundaries are in good agreement with experimental results.



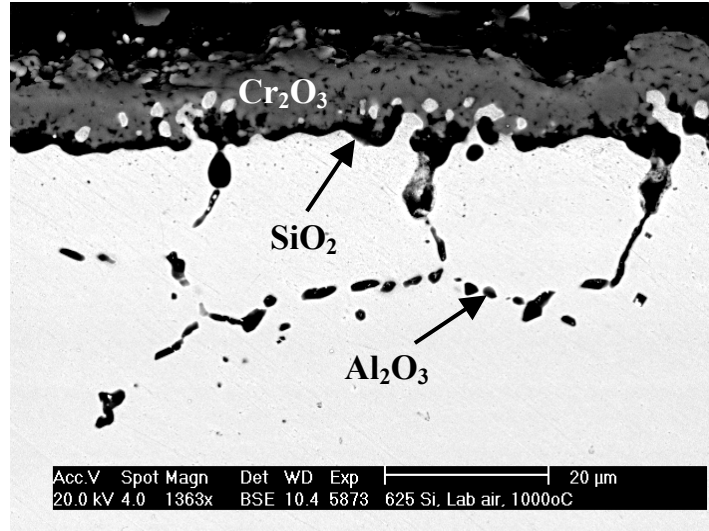
(a)



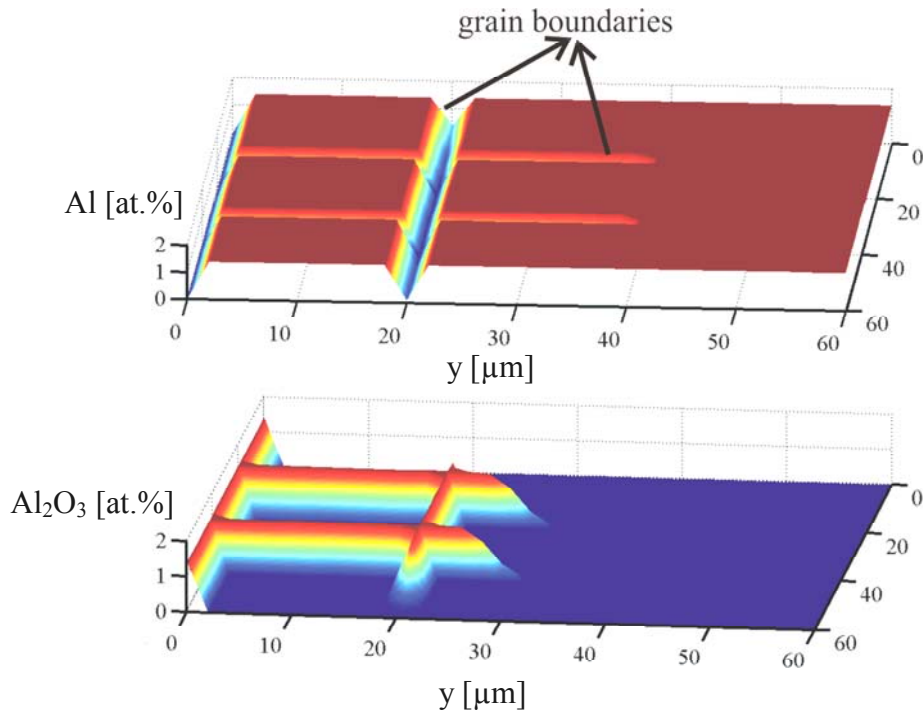
(b)

Figure 3. Initial stage of carbide formation in austenitic steel at 850°C during exposure to an He atmosphere containing 1vol% of methane for 10h: (a) cross section and (b) simulated concentration profiles.

The high Cr concentration in the alloy IN625 cause the formation of an external chromium oxide scale ( $\text{Cr}_2\text{O}_3$ ) during exposure to an oxidizing atmosphere at temperature range between 850°C and 1000°C. Beside the superficial  $\text{Cr}_2\text{O}_3$  scale, internal oxides can be observed (see Fig. 4a). The internal oxidation zone is composed of intergranular aluminum oxide ( $\text{Al}_2\text{O}_3$ ). Simulation of this internal oxidation process is shown in Fig. 4b. Aluminum depletion along grain boundaries as a consequence of aluminum oxide formation is clearly demonstrated by faster diffusion of oxygen along alloy grain boundaries.



(a)

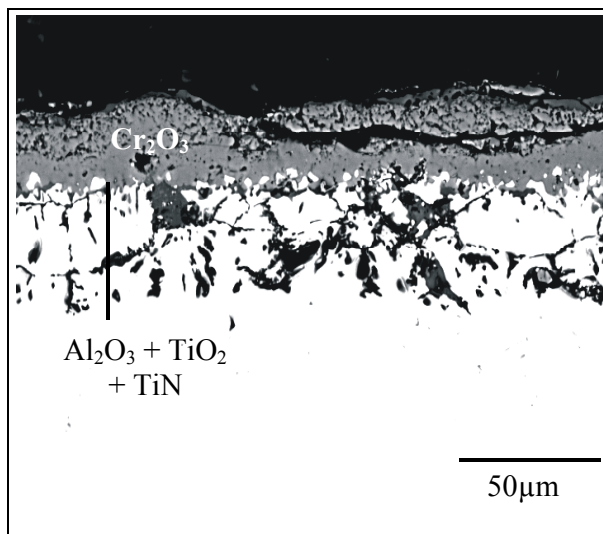


(b)

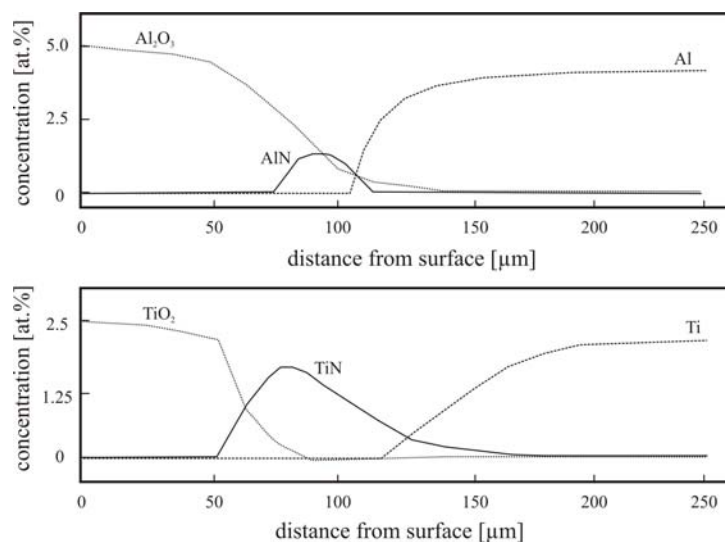
Figure 4.  $\text{Cr}_2\text{O}_3$  scale and internal oxidation zone ( $\text{Al}_2\text{O}_3$ ) formed during exposure of the alloy IN625 to laboratory air at 1000°C: (a) cross section observation and (b) simulated concentration profile of intergranular  $\text{Al}_2\text{O}_3$  formation.

During exposure of the Ni-base alloys Nicrofer7520Ti to an atmosphere containing nitrogen can cause diffusion of dissolved nitrogen into the alloy leading to the formation of nitrides, e.g., TiN, AlN, CrN and  $\text{Cr}_2\text{N}$ . However, the formation of chromium nitrides occurs only for high nitrogen partial pressures and Cr concentrations [ ]. Figure 5a shows the formation of an internal corrosion zone (oxidation+nitridation) formed in Nicrofer7520Ti exposed to laboratory air at 1000°C. The thermodynamically most stable nitride (TiN) was formed on the reaction front while the less stable nitride (AlN) was formed near to the sample surface as observed by Krupp et. al. (2000). Due to the presence of oxygen in the atmosphere, both nitrides and oxides are formed, according to their thermodynamic stabilities. By computer simulation the simultaneous formation of oxides and nitrides and their respective sequence of formation could be shown in Fig. 5b.





(a)



(b)

Figure 5. Corrosion of the Ni-base alloy Nicrofer7520Ti at 1000°C after 100h of exposure to laboratory air: (a) simultaneous formation of oxides and nitrides and (b) one-dimensional simulated concentration profiles of the species involved in the corrosion process.

## 6. Conclusions

In this paper, a computer-based simulation was introduced and applied for three industrial relevant systems, namely, (i) oxidation of low-chromium ferritic steels, (ii) carburization of austenitic steels, and (iii) simultaneous internal nitridation and oxidation of Ni-base superalloys. The versatility of the developed simulation tool allows to perform complex thermodynamic equilibrium calculations by means of the thermodynamic subroutine ChemApp, which is coupled with diffusion calculations. The diffusion differential equation was solved for one- and two-dimensional cases using the MATLAB environment. Diffusion along grain boundaries was separated from that in the bulk of the alloy. A very good agreement between experimental observations and simulation results has proven the high performance of the computer modeling. Therefore, it can be applied for prediction of service life of metallic components used in different atmospheres at high-temperatures as well as for materials selection.

## 7. Acknowledgements

This research has been supported by the EU project OPTICORR and by the Brazilian Research Foundation (CAPES) through a fellowship to one of the authors (V. B. Trindade).

## 8. References

- Birks, N., Meier, G.H., 1983, "Introduction to High Temperature Oxidation of Metals", Ed. Edward Arnold Ltd., London.
- Crank, J., 1986, "The Mathematics of Diffusion", Ed. Clarendon Press, Oxford.
- Grabke, H.J., 1998, "Thermodynamics, mechanisms and kinetics of metal dusting", *Materials and Corrosion*, Vol. 49, pp. 303-308.
- Kofstad, P., 1966, "High Temperature Oxidation of Metals", Ed. Electrochemical Society, London.
- Krupp, U., Christ, H. -J., 2000, "Selective Oxidation and Internal Nitridation during High-Temperature Exposure of Single-Crystalline Nickel-Base Superalloys", *Metallurgical and Materials Transactions*, Vol. 31A, pp.47-56.
- Krupp, U., Trindade, V.B., Schmidt, P., Christ, H.J., Buschmann, U., Wiechert, W., 2005, "Oxidation Mechanism of Cr-Containing Steels and Ni-Base Alloys at High-Temperatures – Part II: Computer-based simulation", *Materials and Corrosion*, in press.
- Trindade, V.B., Krupp, U., Wagenhuber, Ph.E.G., Christ, H.J., 2005, "Oxidation Mechanism of Cr-Containing Steels and Ni-Base Alloys at High-Temperatures – Part I: The different role of alloy grain boundaries", *Materials and Corrosion*, in press.

## 9. Responsibility notice

The authors are the only responsible for the printed material included in this paper.